

Solving the Grad-Shafranov equation using spectral elements for tokamak equilibrium with toroidal rotation

Haolong Li

CAS Key Laboratory of Geospace Environment and Department of Engineering and Applied Physics, University of Science and Technology of China, Hefei, Anhui 230026, China

Ping Zhu*

International Joint Research Laboratory of Magnetic Confinement Fusion and Plasma Physics, State Key Laboratory of Advanced Electromagnetic Engineering and Technology, School of Electrical and Electronic Engineering, Huazhong University of Science and Technology, Wuhan, Hubei 430074, China

Department of Engineering Physics, University of Wisconsin-Madison, Madison, Wisconsin 53706, USA

Abstract

The Grad-Shafranov equation is solved using spectral elements for tokamak equilibrium with toroidal rotation. The Grad-Shafranov solver builds upon and extends the NIMEQ code [Howell and Sovinec, *Comput. Phys. Commun.* 185 (2014) 1415] previously developed for static tokamak equilibria. Both geometric and algebraic convergence are achieved as the polynomial degree of the spectral-element basis increases. A new analytical solution to the Grad-Shafranov equation is obtained for Solov'ev equilibrium in presence of rigid toroidal rotation, in addition to a previously obtained analytical solution for a different set of equilibrium and rotation profiles. The numerical solutions from the extended NIMEQ are benchmarked with the analytical solutions, with good agreements. Besides, the extended NIMEQ code is benchmarked with the FLOW code [L. Guazzotto, R. Betti, et al., *Phys. Plasma* 11(2004)604].

Keywords: Magnetohydrodynamic equilibrium, Grad-Shafranov equation, NIMEQ, NIMROD, toroidal rotation, tokamak

*Corresponding author

Email address: zhup@hust.edu.cn (Ping Zhu)

1. Introduction

For the static equilibrium, the magnetohydrodynamic (MHD) equations yield nonlinear second order differential equation known as Grad-Shafranov equation[1, 2]. The steady state equilibria defined by the solutions of Grad-Shafranov (GS)[1, 2] equation act as the foundation for evaluating the MHD stability of tokamak plasma. Numerical codes have been developed based on different algorithms to solve nonlinear GS equation for given plasma density, temperature and magnetic field profiles directly from experiment[3, 4]. However, most of these codes have only considered the static tokamak equilibrium where plasma flow such as the toroidal rotation is absent.

Toroidal rotation plays significant roles in many tokamak plasma processes. For example, plasma flow and flow shear above certain threshold may lead to the formations of H-mode and internal transport barrier (ITB)[5, 6, 7]. Meanwhile, plasma flow and flow shear can also directly affect plasma stability and transport[8, 9, 10, 11, 12, 13]. In particular, flow shear may have stabilizing effects on neoclassical tearing modes(NTMs)[14, 15], tearing modes (TMs)[16, 17, 18, 19] and edge localized modes(ELMs)[20, 12, 21, 22]. It is found that sufficient toroidal flow opens up a stability window for resistive wall mode (RWM)[23, 24, 25, 26, 11]. On the other hand, plasma flow and shear can also directly modify plasma equilibrium due to the centrifugal effect.

There is a rich history of analytic solution to the GS equation[27, 28, 29, 30, 31, 32, 33]. For example, the solution of the GS homogeneous equation is given by S. B. Zheng[27]. The inhomogeneous GS equation with linear source function P and F known as Solov'ev equilibrium can be solved analytically for any two parameters[27, 28]. The solution to the GS equation with parabolic source functions has been also reported, which allow independent specifications of plasma current density, pressure ratio and one shape moment such as the internal inductance[29, 30]. Besides tokamak, equilibria of other configurations

also have been obtained analytically, such as those of the field-reversed configuration (FRC)[31, 32].

However, the equilibria that can be described using analytic solutions of the GS equation are limited. The GS equation often has to be solved numerically, based on the choice of either the flux along the boundary or the source functions. Fixed-boundary solvers specify the flux value along the boundary of the computation domain. Free-boundary solvers self-consistently calculate the flux value along the boundary of computation, combining the contribution from external magnetic coils and the contribution from the internal plasma current. Various numerical methods have been applied to solving the GS equation, for example, finite difference[34], spectral methods[35], Green's functions[36], linear finite elements[37, 38], and Hermite cubic finite elements[39]. Consequently, many numerical toroidal equilibrium codes have been developed, such as EFIT[4], CHEASE[3], ESC[40], NIMEQ[41], etc.

In addition, several codes are able to solve for toroidal equilibrium in the presence of flow, such as FLOW[8], CLIO[42] and FINESSE[43]. But these codes are often designed for topologically toroidal domains and do not consider the regularity issues associated with the R^{-1} singularity, where R is the major radius. This issue would arise in topologically cylindrical domains, which include the geometric axis $R = 0$.

Previously, a Grad-Shafranov solver NIMEQ[41] was developed for static toroidal equilibrium within the framework of NIMROD[44]. In this work, we extend the Grad-Shafranov solver NIMEQ[41] to the solution of the toroidal equilibrium in the presence of toroidal rotation. A new analytical solution of the modified Grad-Shafranov equation is found. The extended NIMEQ is benchmarked with the new analytical solution and the analytical solution by Maschke and Perrine[45]. The convergence of the extended NIMEQ is tested with h-refinement and p-refinement methods. Furthermore, the extended NIMEQ is benchmarked with FLOW in a convergence study.

The rest of this paper is organized as follows. Section (2) reviews the Grad-Shafranov equation with toroidal rotation. Section (3) shows a new analytical

solution to the modified Grad-Shafranov equation along with the analytical solution obtained by Maschke and Perrin[45]. Section (4) presents the numerical algorithm of the extended NIMEQ. Benchmarking and convergence studies are performed with these two equilibria in section (5). Finally, section (6) gives conclusion and discussion.

2. Grad-Shafranov equation with toroidal rotation

Tokamak equilibria with toroidal rotation are governed by four equations: the force balance equation, magnetic divergence constraint, Ampere's law and state equation of ideal gas[46]

$$\rho(\vec{u} \cdot \nabla)\vec{u} = -\nabla P + \vec{J} \times \vec{B} \quad (1)$$

$$\nabla \cdot \vec{B} = 0 \quad (2)$$

$$\mu_0 \vec{J} = \nabla \times \vec{B} \quad (3)$$

$$P = \frac{\rho}{m_i} T \quad (4)$$

where $\vec{u} = R^2 \Omega \nabla \phi$ denotes the toroidal flow velocity, Ω the frequency of toroidal rotation, P the plasma pressure, \vec{J} the plasma current density, \vec{B} the magnetic field and μ_0 the permeability of vacuum. Besides, ρ denotes the mass density, defined as $\rho \equiv m_i n_i + m_e n_e \simeq m_i n$, $n \equiv n_i = n_e$ and T denotes the plasma temperature defined as $T \equiv T_i + T_e$, where $m_i(m_e)$, $n_i(n_e)$ and $T_i(T_e)$ are the ion (electron) mass, number density and temperature.

The magnetic field is expressed as $\vec{B} = \nabla \phi \times \nabla \psi + F \nabla \phi$ and the plasma current is expressed as $\mu_0 \vec{J} = \mu_0 R J_\phi \nabla \phi + \nabla F \times \nabla \phi$ in the cylindrical coordinate system and $F(\psi) = R B_\phi$ is a flux function [41]. From the curl of Ohm's law, it is observed that the frequency of toroidal rotation is a flux function $\Omega = \Omega(\psi)$. Substituting these above expressions for \vec{B} , \vec{J} and \vec{u} into Eq.(1) yields:

$$\rho R \Omega^2 - \frac{\partial P}{\partial R} = 0 \quad (5)$$

$$\Delta^* \psi = -R^2 \frac{\partial P}{\partial \psi} - F \frac{dF}{d\psi} \quad (6)$$

where the Grad-Shafranov operator is defined as

$$\Delta^* \equiv R \frac{\partial}{\partial R} R^{-1} \frac{\partial}{\partial R} + \frac{\partial^2}{\partial Z^2} \quad (7)$$

For fusion plasma the thermal conduction along magnetic field lines is fast compared to the heat transport perpendicular to a magnetic surface. Thus, plasma temperature can be considered as a flux function, namely $T = T(\psi)$. From Eq.(5), the pressure is integrated as:

$$P(\psi, R) = P_0(\psi) \exp \left[\frac{m_i \Omega^2 R_0^2}{2T} \left(\frac{R^2}{R_0^2} - 1 \right) \right] \quad (8)$$

Substituting $P(\psi, R)$ into Eq.(6), we have

$$\begin{aligned} \Delta^* \psi = & -F \frac{dF}{d\psi} - \mu_0 R^2 \left[\frac{dP_0}{d\psi} - P_0 \frac{m_i R_0^2 \Omega}{T} \left(\frac{R^2}{R_0^2} - 1 \right) \frac{d\Omega}{d\psi} \right. \\ & \left. + P_0 \frac{m_i R_0^2 \Omega^2}{2T^2} \left(\frac{R^2}{R_0^2} - 1 \right) \frac{dT}{d\psi} \right] \exp \left[\frac{m_i \Omega^2 R_0^2}{2T} \left(\frac{R^2}{R_0^2} - 1 \right) \right] \end{aligned} \quad (9)$$

where R_0 denotes the position of magnetic axis. $P = P_0(\psi)$ when $\Omega = 0$. In the limit $\Omega \rightarrow 0$, the static equilibrium pressure can be recovered as a flux function. Meanwhile, Eq.(9) will reduce to the static GS equation.

3. Analytical solutions

3.1. Solov'ev equilibrium with toroidal rotation

We obtain a new analytical solution to Eq.(9) for Solov'ev equilibrium in presence of toroidal rotation. In Solov'ev equilibrium, we assume that:

$$\mu_0 P'_0 = p_1 \quad (10)$$

$$FF' = F_0 \quad (11)$$

where p_1 and F_0 are constants[47]. Furthermore, the plasma temperature and frequency of toroidal rotation are assumed to be constants T_0 and Ω_0 respectively, i.e. $T = T_0$, $\Omega = \Omega_0$

The Grad-Shafranov equation Eq.(9) is reduced to

$$\Delta^* \psi = -p_1 R^2 \exp[M_0^2(\frac{R^2}{R_0^2} - 1)] - F_0 \quad (12)$$

where $M_0 = \frac{m_i R_0^2 \Omega_0^2}{2T_0}$ denotes the Mach number at $R = R_0$.

The solution of Eq.(12) is of the form $\psi(R, Z) = \psi_p(R, Z) + \psi_h(R, Z)$, where ψ_p is the particular solution and ψ_h is the homogeneous solution[47, 27].

$$\psi_h = c_1 + c_2 R^2 + c_3(R^4 - 4R^2 Z^2) + c_4[R^2 \ln(R) - Z^2] \quad (13)$$

where these constants c_1, c_2, c_3, c_4 are determined by boundary condition. Then, for a particular solution:

$$\psi_p = -p_1 \left(\frac{R_0^2}{2M_0^2} \right)^2 \left\{ \exp \left[M_0^2 \left(\frac{R^2}{R_0^2} - 1 \right) \right] - \frac{M_0^2}{R_0^2} (R^2 - R_0^2) - 1 \right\} - \frac{F_0}{2} Z^2 \quad (14)$$

We obtain a new analytical solution of Grad-shafranov equation for the Solov'ev equilibrium with toroidal rotation:

$$\begin{aligned} \psi = \psi_p + \psi_h = c_1 + c_2 R^2 + c_3(R^4 - 4R^2 Z^2) + c_4[R^2 \ln(R) - Z^2] \quad (15) \\ - p_1 \left(\frac{R_0^2}{2M_0^2} \right)^2 \left\{ \exp \left[M_0^2 \left(\frac{R^2}{R_0^2} - 1 \right) \right] - \frac{M_0^2}{R_0^2} (R^2 - R_0^2) - 1 \right\} - \frac{F_0}{2} Z^2 \end{aligned}$$

This solution reduces to the solution of static Solov'ev equilibrium when $\Omega_0 \rightarrow 0$ or $M_0 \rightarrow 0$.

$$\psi = \lim_{M_0 \rightarrow 0} \psi_h + \psi_p = \psi_h + \lim_{M_0 \rightarrow 0} \psi_p = \psi_h - p_1 \frac{(R^2 - R_0^2)^2}{8} - \frac{F_0}{2} Z^2 \quad (16)$$

The above solution in Eq.(16) was a specific case of the Grad-Shafranov equation solutions obtained before in Ref.[27]. A similar solution of Solov'ev equilibrium with rigid toroidal rotation was recently obtained by Chu et al[48],

$$\psi = \psi_h - p_1 \left(\frac{R_0^2}{2M_0^2} \right)^2 \left\{ \exp \left[M_0^2 \left(\frac{R^2}{R_0^2} - 1 \right) \right] - \frac{M_0^2}{R_0^2} (R^2 - R_0^2) - 1 \right\} - \frac{F_0}{2} Z^2 + \frac{1 - 2\beta_{pJ}}{16} \left[\left(\frac{R^2}{R_0^2} - 1 \right)^2 - \frac{4R^2 Z^2}{R_0^4} \right] \quad (17)$$

where $\beta_{pJ} = -\frac{R_0^2 p_1}{F_0 + R_0^2 p_1}$. The two solutions in Eqs.(15) and (17) differ only in the last term with the factor of $\frac{1-2\beta_{pJ}}{16}$.

3.2. Maschke-Perrin Equilibrium

Another analytic solution of Eq.(6) was previously found based on the following assumptions[45]:

$$P = \frac{P_0}{R_L^4} (\psi - \psi_1) \exp(\gamma R^2 \Omega^2 / 2R_L^2) \quad (18)$$

$$F^2 = F_0^2 + 2 \frac{M}{R_L^2} (\psi - \psi_1) \quad (19)$$

$$\frac{\omega^2}{RT} = \text{constant} = \gamma \frac{\Omega^2}{R_L^2} \quad (20)$$

where γ is the ratio of specific heats and R_L, P_0, ψ_1, F_0, M are constants.

In case of $M = 0$, the analytical solution takes the form

$$\begin{aligned} \psi - \psi_1 &= CP_0 \frac{R^2}{R_L^2} \\ &+ P_0 \left\{ \frac{(\epsilon_a - 1)}{4} \left(\frac{Z^2}{R_L^2} - \frac{R^2}{4R_L^2} \right) \frac{R^2}{R_L^2} \right. \\ &\left. + \frac{1}{\gamma^2 \Omega^4} \left[1 + \frac{\gamma \Omega^2 R^2}{2R_L^2} - \exp \left(\frac{\gamma \Omega^2 R^2}{2R_L^2} \right) \right] \right\} \end{aligned} \quad (21)$$

where $C = \frac{(\epsilon_a - 1)}{8} r_a^2 + \frac{1}{2\gamma \Omega^2} \left[\exp \left(\frac{\gamma \Omega^2 r_a^2}{2} - 1 \right) \right]$ is a constant, ϵ_a is a constant related to the ellipticity of the plasma cross-section, $r_a = R_0/R_L$ denotes the ratio between the position of magnetic axis R_0 and the chosen scale length R_L .

4. Numerical algorithm

NIMEQ solves the Grad-Shafranov equation in weak form using Galerkin formulation[41]. Defining one scalar field $\Lambda = \psi/R^2$, the Grad-Shafranov operator can be transformed into a divergence of a vector, $\Delta^*\psi = \nabla \cdot R^2\nabla\Lambda$. The scalar field Λ can be spilt into two parts: Λ_0 and Λ_h where Λ_0 satisfies the specified inhomogeneous boundary condition for Λ and Λ_h satisfies the boundary condition $\Lambda_h = 0$. The Λ_h is expanded onto a series of C^0 spectral element basis functions $\Lambda_h = \sum_i \Lambda_i \alpha_i$. The weak form of Grad-Shafranov equation is obtained as:

$$\begin{aligned} & \sum_i \Lambda_i \int dV R^2 \nabla \alpha_i \cdot \nabla \alpha_j = \\ & \int dV \left\{ FF' + \mu_0 R^2 \left[\frac{dP_0}{d\psi} + P_0 \frac{m_i R_0^2 \Omega}{T} \left(\frac{R^2}{R_0^2} - 1 \right) \frac{d\Omega}{d\psi} - P_0 \frac{m_i R_0^2 \Omega^2}{2T^2} \left(\frac{R^2}{R_0^2} - 1 \right) \frac{dT}{d\psi} \right] \right. \\ & \left. \exp \left[\frac{m_i \Omega^2 R_0^2}{2T} \left(\frac{R^2}{R_0^2} - 1 \right) \right] \right\} \alpha_j - \int dV R^2 \nabla \Lambda_0 \cdot \nabla \alpha_j \end{aligned} \quad (22)$$

For compactness, Eq.(22) is written as $M\Lambda = Q$. The modified Picard iterations in Eq.(23), has been applied to solve the Grad-Shafranov equation in NIMEQ, where $\theta \in (0, 1]$ denotes the relaxation parameter to achieve convergence.

$$M\Lambda^n = (1 - \theta)M\Lambda^{n-1} + \theta Q^{n-1} \quad (23)$$

After iteration, these equilibrium fields are calculated from the converged solution for Λ . The pressure, temperature, toroidal flow velocity \vec{u}_ϕ and RB_ϕ values are calculated from the prescribed $P_0(\psi)$, $F(\psi)$, $T(\psi)$, $\Omega(\psi)$ using the converged solution $\Lambda(R, Z)$ through Eq.(8) and $\vec{u}_\phi = R^2\Omega(\psi)\nabla\phi$. The poloidal magnetic field is expressed as Eq.(24) in terms of Λ .

$$\vec{B}_p = \frac{1}{R} \hat{e}_\phi \times (2R\hat{e}_R\Lambda + R^2\nabla\Lambda) \quad (24)$$

where \hat{e}_R and \hat{e}_ϕ represent the unit vectors in the R and ϕ directions respectively.

The poloidal current is calculated directly from the magnetic field through the relation $\vec{J}_p = -F' \vec{B}_p / \mu_0$. And the toroidal current density is calculated using Eq.(25)

$$J_\phi = \frac{1}{\mu_0 R} \Delta^* \psi = R \frac{\partial P}{\partial \psi} + \frac{1}{\mu_0 R} F \frac{dF}{d\psi} \quad (25)$$

5. Benchmark and Convergence

The analytic solutions in section 3.1 are plotted in a domain of rectangular poloidal cross section with $4.5 < R < 5.5$ and $-0.5 < Z < 0.5$ (Fig.1). Parameters are set as $p_1 = -8.0 \times 10^{-2}$, $F_0 = 20$, $M_0 = 6.1$ and the poloidal flux along the boundary is prescribed using Eq.(15), with $c_1 = -104.1301$, $c_2 = 10.6087$, $c_3 = 0.0015$ and $c_4 = -5.2103$. The equilibrium poloidal flux contours for Solov'ev equilibrium with toroidal rotation and without toroidal rotation presented in Fig.1 show modification induced by toroidal rotation.

Similarly, the equilibrium poloidal flux contours for Maschke and Perrin's equilibrium in section 3.2 are plotted in a domain of rectangular poloidal cross section with $4.5 \leq R \leq 5.5$ and $-0.5 \leq Z \leq 0.5$ (Fig.2). In this case, we choose $\epsilon_a = 0$, $\gamma = 5/3$, $R_0 = R_L = 5.0$, $P_0 = -0.1 \times R_L^4$, $\Omega = 3.0 \times 10^5$, $\psi_0 = 0$ and $\epsilon_a = 0$. Distortion of flux surfaces due to toroidal rotation is also apparent.

Both benchmark and convergence studies are performed for Solov'ev equilibrium and Maschke and Perrin's equilibrium by comparing the numerical and analytical solutions. The numerical error of equilibrium poloidal flux is defined as $E_n = \sqrt{\sum (\psi_n - \psi_a)^2 / \sum \psi_a^2}$, where ψ_n is the numerical solution from the extended NIMEQ and ψ_a is the analytic solution from Eq.(15) and Eq.(21). And the summation is performed over all of the finite-element nodes.

Two methods, i.e. h-refinement and p-refinement, are applied to checking the convergence of the extended NIMEQ in both equilibria. In the p-refinement method, the polynomial degree of each element is increased whereas the number of elements is kept constant. H-refinement maintains the polynomial degree of

the elements while increasing the number of elements. The decaying rate of the error for a smooth solution of a second order differential equation is bounded by the asymptotic rate of convergence $h^{(p+1)}$ for sufficiently smooth solutions, where h is a characteristic element length of calculation region and p is the polynomial degree[49].

We use meshes with equal numbers of elements in the radial and vertical directions. In the p-refinement study, the polynomial degree of elements is scanned from 2 to 15 when keeping the 2×2 and 10×10 element meshes fixed for both equilibria. In both equilibrium cases, the numerical errors decay linearly to a minimum value, which indicates geometric convergence in Fig.3 and Fig.5 [49]. The numerical error in 10×10 element meshes decays faster than that in 2×2 element meshes in both equilibria.

In h-refinement study, the number of elements are scanned from 4 to 94 when polynomial degree of elements keeps 2 and 4. In h-refinement studies of both equilibrium cases, the numerical errors decay linearly to a minimum value, indicating algebraic convergence in Fig.4 and Fig.6[49]. The decay rate of numerical errors with polynomial degree fixed 4 is larger than that with polynomial degree fixed 2. The blue lines in both figures stand for the scaling N^{-3} and N^{-6} fitted from the decaying numerical errors, where N denotes the number of elements. Both figures show that the decay rates of numerical error in ψ are between $p+1$ and $p+2$.

FLOW is a finite difference code, which solves the Bernoulli-Grad-Shafranov equations for tokamak the equilibriums with flow[8]. The extended NIMEQ is benchmarked with the FLOW code here. The comparison is performed in a poloidal domain of $2.0 \leq R \leq 4$ and $-1.0 \leq Z \leq 1.0$. The F and Ω are chosen as constants. And the pressure profile is specified as one quadratic function of the normalized ψ , $P_0(\psi) = P_{\text{open}} + P_1(1 - \psi) + 4P_2\psi(\psi - 1)$. The number density profile is similar to the pressure profile, since $n(\psi) = \frac{P_0(\psi)}{P_0(0)}n_{\text{axis}}$, where $P_0(0)$ and n_{axis} denote the pressure and number density on magnetic axis. This number density profile is thus chosen so as to obtain a constant temperature. The Mach number is constant and equals 0.3. The overlay of

ψ from the extended NIMEQ and FLOW is shown in Fig.7. For comparison, the relatively numerical error is defined as $\sqrt{\sum(\psi_{\text{FLOW}} - \psi_{\text{NIMEQ}})^2 / \sum \psi_{\text{NIMEQ}}^2}$ where ψ_{NIMEQ} denotes the numerical solution from NIMEQ and ψ_{FLOW} denotes the numerical solution from FLOW. Because the computation grids are different in NIMEQ and FLOW, the bi-cubic spline interpolation is applied to calculation of relatively numerical error. The relative numerical error decreases with the computation grid point number (Fig.8).

6. Conclusion and discussion

We have extended NIMEQ by solving the modified Grad-Shafranov equation that self-consistently takes into account of the effects of toroidal rotation. A new analytic solution to the modified Grad-Shafranov equation is obtained for the Solov'ev equilibrium in presence of a rigid toroidal rotation. Both the new analytical solution and the Maschke-Perrin equilibrium are used in benchmark and convergence studies. High accuracy solution with numerical error to the order of 10^{-10} or smaller is achieved. The extended NIMEQ is also successfully benchmarked with the FLOW code.

Next we plan to extend the modified Grad-Shafranov equation to include free boundary condition, and to study the effects on equilibrium profiles due to toroidal rotation. Meanwhile, the poloidal flow can be also included in the extended NIMEQ to calculate equilibrium in presence of arbitrary flows.

Acknowledgments

This work was supported by the Fundamental Research Funds for the Central Universities at Huazhong University of Science and Technology Grant No. 2019kfyXJJS193, the National Natural Science Foundation of China Grant No. 11775221, the National Magnetic Confinement Fusion Science Program of China Grant No. 2015GB101004, and U.S. Department of Energy Grant Nos. DE-FG02-86ER53218 and de-sc0018001. This research used the com-

puting resources from the Supercomputing Center of University of Science and Technology of China.

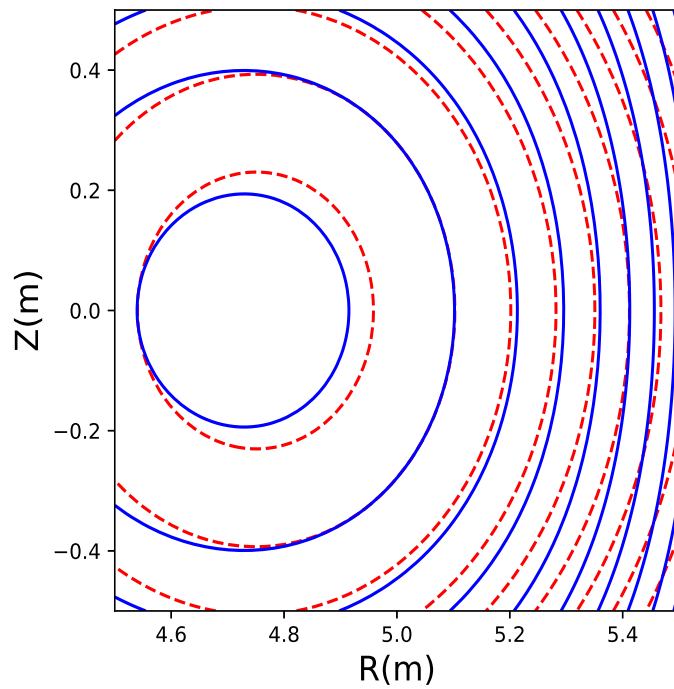


Figure 1: The poloidal flux contour of the Solov'ev equilibrium with $p_1 = -8.0 \times 10^{-2}$, $F_0 = -20$ and $M_0 = 4$. The red dashed lines stand for the equilibrium without toroidal rotation. The blue solid lines stand for the equilibrium with toroidal rotation.

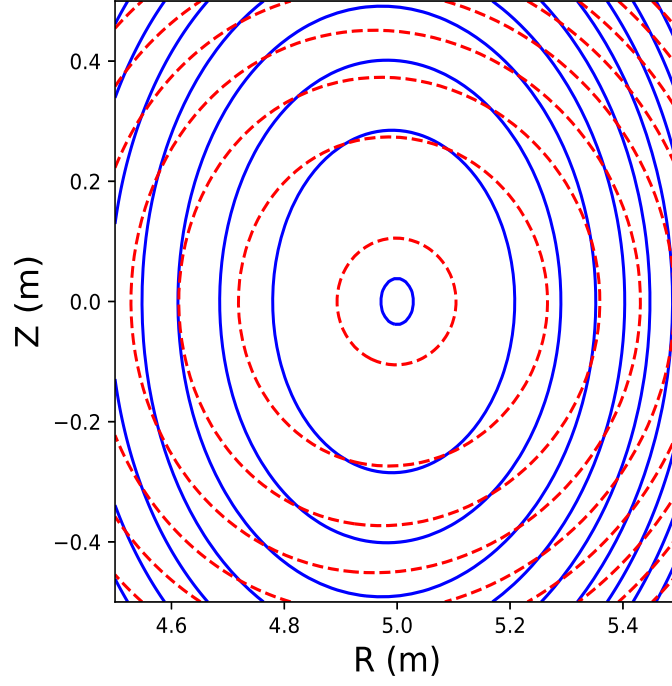


Figure 2: The poloidal flux contour of the Maschke and Perrin's equilibrium with $P_0 = -8.0 \times 10^{-3} \times R_L^4$ and $\Omega = 5.0 \times 10^4$. The red dashed lines stand for the equilibrium without toroidal rotation. The blue solid lines stand for the equilibrium with toroidal rotation.

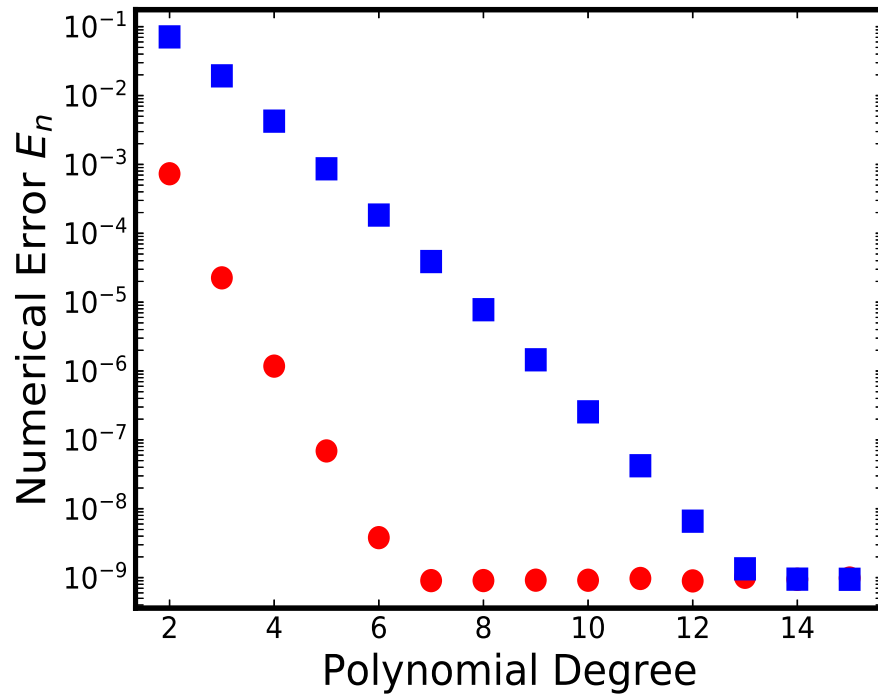


Figure 3: The numerical error E_n of ψ as a function of the element polynomial degree for 2×2 element mesh (■) and 10×10 element mesh (●) in the case of Solov'ev equilibrium with toroidal rotation.

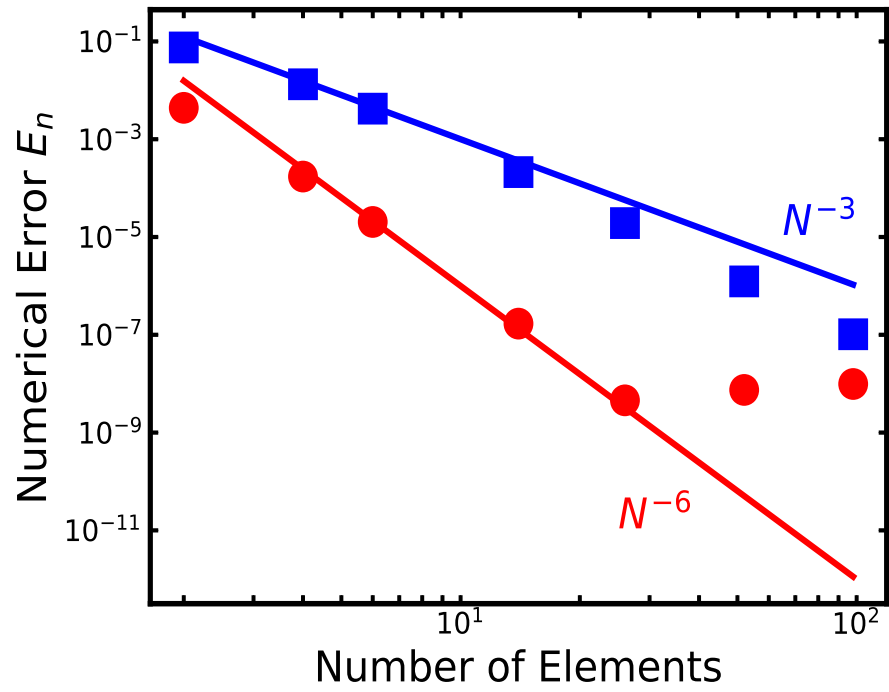


Figure 4: The numerical error E_n of ψ as a function of the element numbers for 2nd order elements (■) and 4th order elements (●) in the case of the Solov'ev equilibrium with toroidal rotation.

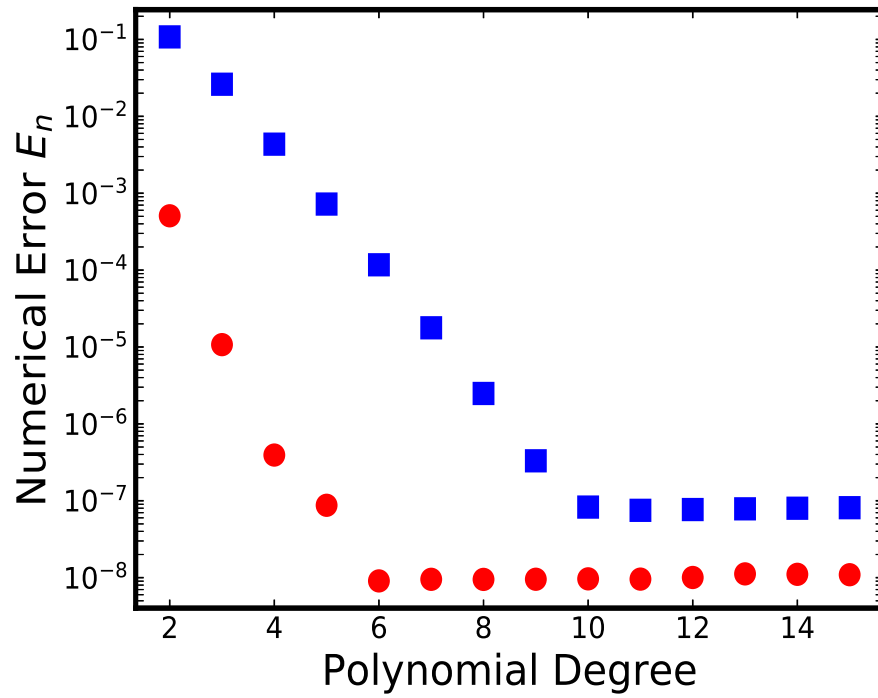


Figure 5: The numerical error E_n of ψ as a function of the element polynomial degree for 2×2 element mesh (■) and 10×10 element mesh (●) in the case of Maschke and Perrin's equilibrium.

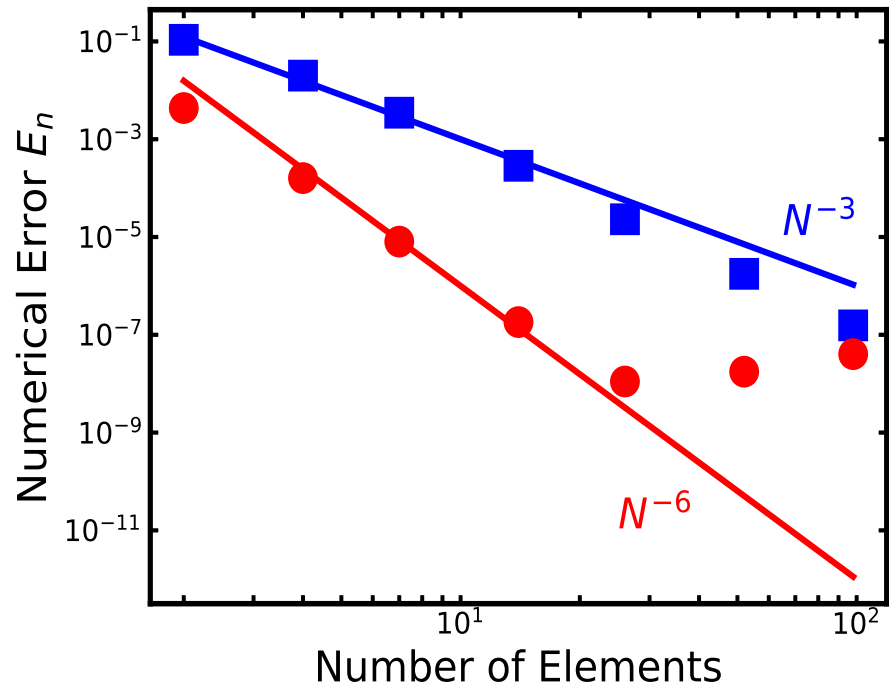


Figure 6: The numerical error E_n of ψ as a function of the element numbers for 2nd order elements (■) and 4th order elements (●) in the case of Maschke and Perrin's equilibrium.

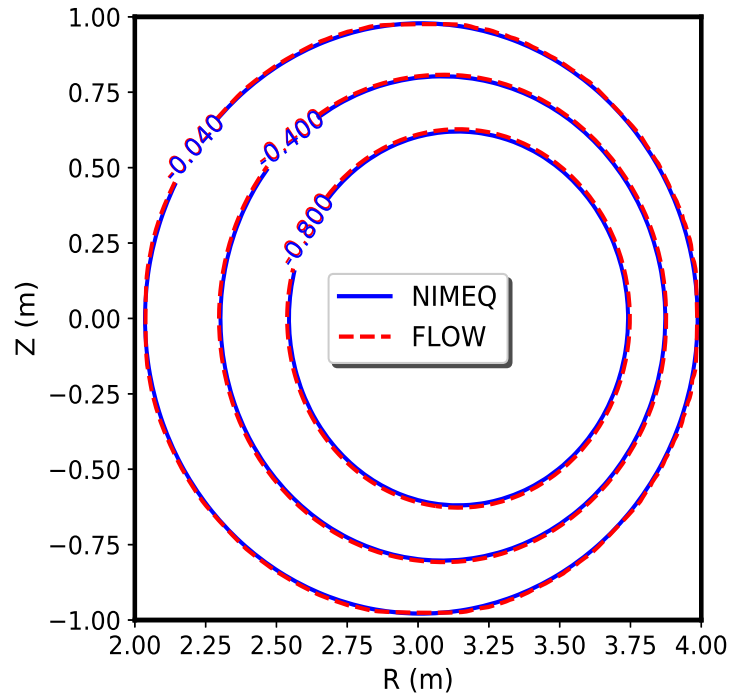


Figure 7: The comparison between ψ from the extended NIMEQ and ψ from FLOW code, with $P_{\text{open}} = 1.0 \times 10^{-3}$, $P_1 = 0.8$, $P_2 = 0.2$, $n_{\text{axis}} = 8.0 \times 10^{19}$ and $F = 4.0$. The red dashed lines stand for the ψ from FLOW code and blue solid lines denote the ψ from the extended NIMEQ.

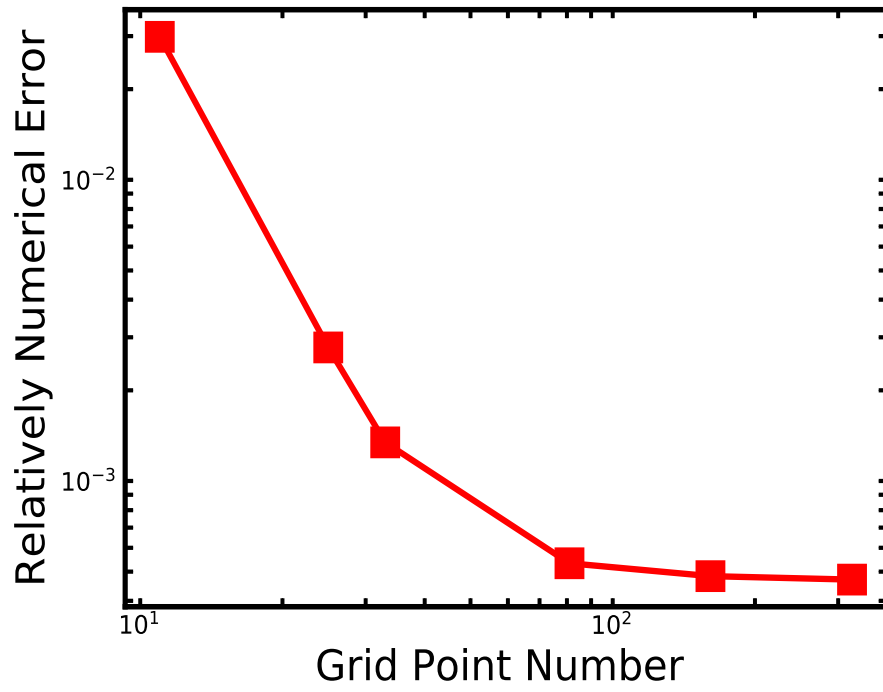


Figure 8: The relatively error as a function of grid point number.

References

- [1] H. Grad, H. Rubin, Hydromagnetic equilibria and force-free fields, *Journal of Nuclear Energy* (1954) 7 (1958) 284–285.
- [2] V. Shafranov, On magnetohydrodynamical equilibrium configurations, *Soviet Physics JETP* 6 (1958) 1013.
- [3] H. Lütjens, A. Bondeson, O. Sauter, The CHEASE code for toroidal MHD equilibria, *Computer physics communications* 97 (1996) 219–260. 00000.
- [4] L. L. Lao, H. E. S. John, Q. Peng, J. R. Ferron, E. J. Strait, T. S. Taylor, W. H. Meyer, C. Zhang, K. I. You, MHD equilibrium reconstruction in the DIII-D tokamak, *Fusion Science and Technology* 48 (2005) 968–977.
- [5] S. Ding, A. M. Garofalo, J. Qian, L. Cui, J. T. McClenaghan, C. Pan, J. Chen, X. Zhai, G. McKee, Q. Ren, X. Gong, C. T. Holcomb, W. Guo, L. Lao, J. Ferron, A. Hyatt, G. Staebler, W. Solomon, H. Du, Q. Zang, J. Huang, B. Wan, Confinement improvement in the high poloidal beta regime on DIII-D and application to steady-state H-mode on EAST, *Physics of Plasmas* 24 (2017) 056114.
- [6] Y. Sakamoto, Y. Kamada, S. Ide, T. Fujita, H. Shirai, T. Takizuka, Y. Koide, T. Fukuda, T. Oikawa, T. Suzuki, K. Shinohara, R. Yoshino, JT-60 Team, Characteristics of internal transport barriers in JT-60U reversed shear plasmas, *Nuclear Fusion* 41 (2001) 865–872.
- [7] P. de Vries, E. Joffrin, M. Brix, C. Challis, K. Crombé, B. Esposito, N. Hawkes, C. Giroud, J. Hobirk, J. Linnroth, P. Mantica, D. Strintzi, T. Tala, I. Voitsekhovitch, Internal transport barrier dynamics with plasma rotation in JET, *Nuclear Fusion* 49 (2009) 075007.
- [8] L. Guazzotto, R. Betti, J. Manickam, S. Kaye, Numerical study of tokamak equilibria with arbitrary flow, *Physics of Plasmas* 11 (2004) 604–614.

- [9] Y. Shi, G. Xu, F. Wang, M. Wang, J. Fu, Y. Li, W. Zhang, W. Zhang, J. Chang, B. Lv, J. Qian, J. Shan, F. Liu, S. Ding, B. Wan, S.-G. Lee, M. Bitter, K. Hill, Observation of cocurrent toroidal rotation in the east tokamak with lower-hybrid current drive, *Phys. Rev. Lett.* 106 (2011) 235001.
- [10] C. C. Hegna, The effect of sheared toroidal rotation on pressure driven magnetic islands in toroidal plasmas, *Physics of Plasmas* 23 (2016) 052514.
- [11] S. Wang, Z. W. Ma, Influence of toroidal rotation on resistive tearing modes in tokamaks, *Physics of Plasmas* 22 (2015) 122504.
- [12] N. Aiba, S. Tokuda, M. Furukawa, P. Snyder, M. Chu, MINERVA: Ideal MHD stability code for toroidally rotating tokamak plasmas, *Computer Physics Communications* 180 (2009) 1282 – 1304.
- [13] X. Yan, P. Zhu, Y. Sun, Neoclassical toroidal viscosity torque in tokamak edge pedestal induced by external resonant magnetic perturbation, *Physics of Plasmas* 24 (2017) 082510.
- [14] R. J. L. Haye, R. J. Buttery, The stabilizing effect of flow shear on $m/n=3/2$ magnetic island width in DIII-D, *Physics of Plasmas* 16 (2009) 022107.
- [15] R. J. Buttery, R. J. L. Haye, P. Gohil, G. L. Jackson, H. Reimerdes, E. J. Strait, the DIII-D Team, The influence of rotation on the β_N threshold for the 21 neoclassical tearing mode in DIII-D, *Physics of Plasmas* 15 (2008) 056115.
- [16] K. P. Wessen, M. Persson, Tearing-mode stability in a cylindrical plasma with equilibrium flows, *Journal of Plasma Physics* 45 (1991) 267–283.
- [17] R. L. Haye, C. Petty, P. Politzer, the DIII-D Team, Influence of plasma flow shear on tearing in DIII-D hybrids, *Nuclear Fusion* 51 (2011) 053013.
- [18] A. Sen, D. Chandra, P. Kaw, Tearing mode stability in a toroidally flowing plasma, *Nuclear Fusion* 53 (2013) 053006.

- [19] R. J. L. Haye, D. P. Brennan, R. J. Buttery, S. P. Gerhardt, Islands in the stream: The effect of plasma flow on tearing stability, *Physics of Plasmas* 17 (2010) 056110.
- [20] S. Cheng, P. Zhu, D. Banerjee, Enhanced toroidal flow stabilization of edge localized modes with increased plasma density, *Physics of Plasmas* 24 (2017) 092510.
- [21] T. Xia, X. Xu, P. Xi, Six-field two-fluid simulations of peeling-ballooning modes using BOUT++, *Nuclear Fusion* 53 (2013) 073009.
- [22] M. Fenstermacher, X. Xu, I. Joseph, M. Lanctot, C. Lasnier, W. Meyer, B. Tobias, L. Zeng, A. Leonard, T. Osborne, Fast pedestal, SOL and divertor measurements from DIII-D to validate BOUT++ nonlinear ELM simulations, *Journal of Nuclear Materials* 438 (2013) S346 – S350. Proceedings of the 20th International Conference on Plasma-Surface Interactions in Controlled Fusion Devices.
- [23] M. S. Chu, J. M. Greene, T. H. Jensen, R. L. Miller, A. Bondeson, R. W. Johnson, M. E. Mauel, Effect of toroidal plasma flow and flow shear on global magnetohydrodynamic MHD modes, *Physics of Plasmas* 2 (1995) 2236–2241.
- [24] D. J. Ward, A. Bondeson, Stabilization of ideal modes by resistive walls in tokamaks with plasma rotation and its effect on the beta limit, *Physics of Plasmas* 2 (1995) 1570–1580.
- [25] S. Gerhardt, D. Brennan, R. Buttery, R. L. Haye, S. Sabbagh, E. Strait, M. Bell, R. Bell, E. Fredrickson, D. Gates, B. LeBlanc, J. Menard, D. Stutman, K. Tritz, H. Yuh, Relationship between onset thresholds, trigger types and rotation shear for the $m/n = 2/1$ neoclassical tearing mode in a high-spherical torus, *Nuclear Fusion* 49 (2009) 032003.
- [26] R. Betti, Beta limits for the $n=1$ mode in rotating-toroidal-resistive plasmas surrounded by a resistive wall, *Physics of Plasmas* 5 (1998) 3615–3631.

- [27] S. B. Zheng, A. J. Wootton, E. R. Solano, Analytical tokamak equilibrium for shaped plasmas, *Physics of Plasmas* 3 (1996) 1176–1178.
- [28] C. Atanasiu, S. Günter, K. Lackner, I. Miron, Analytical solutions to the Grad-Shafranov equation, *Physics of Plasmas* 11 (2004) 3510–3518.
- [29] P. J. Mc Carthy, Analytical solutions to the Grad-Shafranov equation for tokamak equilibrium with dissimilar source functions, *Physics of Plasmas* 6 (1999) 3554–3560.
- [30] S. Šesnić, D. Poljak, E. Slišković, A review of some analytical solutions to the Grad-Shafranov equation, in: 2014 22nd International Conference on Software, Telecommunications and Computer Networks (SoftCOM), IEEE, 2014, pp. 24–27.
- [31] P. Parks, M. Schaffer, Analytical equilibrium and interchange stability of single-and double-axis field-reversed configurations inside a cylindrical cavity, *Physics of Plasmas* 10 (2003) 1411–1423.
- [32] H. L. Berk, J. H. Hammer, H. Weitzner, Analytic field-reversed equilibria, *Physics of Fluids* 24 (1981) 1758–1759.
- [33] S. Wang, Theory of tokamak equilibria with central current density reversal, *Phys. Rev. Lett.* 93 (2004) 155007.
- [34] J. Johnson, H. Dalhed, J. Greene, R. Grimm, Y. Hsieh, S. Jardin, J. Manickam, M. Okabayashi, R. Storer, A. Todd, D. Voss, K. Weimer, Numerical determination of axisymmetric toroidal magnetohydrodynamic equilibria, *Journal of Computational Physics* 32 (1979) 212 – 234.
- [35] K. Ling, S. Jardin, The princeton spectral equilibrium code: PSEC, *Journal of Computational Physics* 58 (1985) 300 – 335.
- [36] L. Lao, H. S. John, R. Stambaugh, A. Kellman, W. Pfeiffer, Reconstruction of current profile parameters and plasma shapes in tokamaks, *Nuclear Fusion* 25 (1985) 1611–1622.

- [37] J. Blum, J. L. Foll, B. Thooris, The self-consistent equilibrium and diffusion code sced, *Computer Physics Communications* 24 (1981) 235 – 254.
- [38] R. Gruber, R. Iacono, F. Troyon, Computation of MHD equilibria by a quasi-inverse finite hybrid element approach, *Journal of Computational Physics* 73 (1987) 168 – 182.
- [39] H. Lütjens, A. Bondeson, A. Roy, Axisymmetric MHD equilibrium solver with bicubic Hermite elements, *Computer Physics Communications* 69 (1992) 287 – 298.
- [40] L. E. Zakharov, A. Pletzer, Theory of perturbed equilibria for solving the Grad-Shafranov equation, *Physics of Plasmas* 6 (1999) 4693–4704.
- [41] E. Howell, C. Sovinec, Solving the Grad-Shafranov equation with spectral elements, *Computer Physics Communications* 185 (2014) 1415 – 1421.
- [42] S. Semenzato, R. Gruber, H. Zehrfeld, Computation of symmetric ideal MHD flow equilibria, *Computer Physics Reports* 1 (1984) 389 – 425.
- [43] A. Beliën, M. Botchev, J. Goedbloed, B. van der Holst, R. Keppens, FINESSE: Axisymmetric MHD equilibria with flow, *Journal of Computational Physics* 182 (2002) 91 – 117.
- [44] C. Sovinec, A. Glasser, T. Gianakon, D. Barnes, R. Nebel, S. Kruger, D. Schnack, S. Plimpton, A. Tarditi, M. Chu, Nonlinear magnetohydrodynamics simulation using high-order finite elements, *Journal of Computational Physics* 195 (2004) 355 – 386.
- [45] E. K. Maschke, H. Perrin, Exact solutions of the stationary MHD equations for a rotating toroidal plasma, *Plasma Physics* 22 (1980) 579.
- [46] F. Masaru, A. Yuji, A. Satoshi, W. Masahiro, Tokamak equilibria with toroidal flows, *Journal of Plasma and Fusion Research* 76 (2000) 937–948.
- [47] L. Solov’ev, The theory of hydromagnetic stability of toroidal plasma configurations, *Sov. Phys. JETP* 26 (1968).

- [48] M. S. Chu, Y. Hu, W. Guo, Generalization of Solovév's approach to finding equilibrium solutions for axisymmetric plasmas with flow, *Plasma Science and Technology* 20 (2018) 035101.
- [49] J. P. Boyd, *Chebyshev and Fourier Spectral Methods*, Second Edition ed., DOVER Publications, Inc., 2000.